*Computers & Structures* Vol. 43, No. 6, pp. 1091–1103, 1992
Printed in Great Britain.

0045-7949/92 $5.00 + 0.00


# SEISMIC ANALYSIS OF ASYMMETRIC BUILDING–FOUNDATION SYSTEMS

K. S. SIVAKUMARAN,† MIN-SHAY LIN‡ and PISIDHI KARASUDHI‡

†Department of Civil Engineering and Engineering Mechanics, McMaster University, Hamilton, Ontario L8S 4L7, Canada

‡Division of Structural Engineering and Construction, Asian Institute of Technology, P.O. Box 2754, Bangkok 10501, Thailand

(*Received* 14 *May* 1991)

**Abstract**—A method of analysis for the earthquake response of three-dimensional multi-storey asymmetric buildings founded on a flexible foundation is presented. The building–foundation system considered in this study is a linear $N$-storey asymmetric building on a rigid footing resting on the surface of a linear elastic half-space. The whole system has $3N + 5$ displacement degrees of freedom. The governing equations are developed considering the motions of each floor and the motions of the whole system. The governing equations of the floors are first uncoupled in terms of footing displacements using the mode superposition method. Substitution of structural deformations, in combination with the dynamic soil–structure interaction force–displacement relationships proposed by Veletsos and Verbic [*ASCE J. Engng Mech. Div.* **100**, 189–201 (1974)] and Veletsos and Nair [*ASCE J. Geotechn. Engng Div.* **100**, 225–246 (1974)] into the governing equations of the whole system results in five integro-differential equations for footing displacements, which are then solved by numerical step-by-step time-history analysis. A 10-storey asymmetric building on soft soil was subjected to an artificially generated earthquake excitation in order to obtain the soil–structure interaction and eccentricity effects. The results show that soft soil conditions increase the lateral deflections, but reduce the twists, storey shears, and torques. Increasing eccentricity increases the twists and torques, but does not modify the lateral deflections at the centre of mass, and the total storey shears.

## INTRODUCTION

Unless the distribution of the floor masses and the distribution of load-resisting elements are symmetric with respect to some orthogonal axes, the buildings are considered to be asymmetric. Asymmetric buildings when subjected to earthquake ground excitations exhibit coupled lateral–torsional movements, due to non-coincident centre of mass (CM) and centre of stiffness (CS). Various studies [1–5] have already been undertaken to establish the seismic response of such torsionally coupled asymmetric buildings. However, these studies [1–5] assumed that the asymmetric structure is supported by a rigid foundation. Since all real materials deform under loads, the rigid foundation assumption represents an approximation to the real conditions.

There are occasions, such as multi-storey buildings founded on soft soil, when it becomes necessary to consider the effects of deformability of the foundation. These effects are generally referred to as soil–structure interaction effects. When the soil–structure interaction effects are included in the analysis of a building, the whole system may be referred to as a building–foundation system. The governing equations of motion for a multi-storey building–foundation system, as well as the methods of solving these equations, are relatively complex. Nevertheless, the effects of soil–structure interaction on the seismic response of multi-storey buildings have been established in the past [6–10]. These studies [6–10], however, were limited to two-dimensional (planar) multi-storey frames, thus the conclusion reached may be applied for symmetric buildings only.

Recently, Sivakumaran [11] presented a method of seismic analysis of mono-symmetric multi-storey building–foundation systems. It appears that a method of seismic analysis of asymmetric multi-storey building–foundtion systems does not exist in the published literature. The objective of this paper is to formulate a method of analysis for the seismic response of three-dimensional asymmetric multi-storey buildings including soil–structure interaction effects.

## METHOD OF ANALYSIS

As shown in Fig. 1, the building–foundation system used in the present study consists of an $N$-storey three-dimensional asymmetric superstructure founded on a rigid footing, which in turn, is supported by a flexible soil mass foundation. Structural asymmetry may arise due to asymmetric distribution of masses or asymmetric distribution of load-resisting elements.

In this study the floor is assumed to be rectangular in plan and the building mass is assumed to be evenly distributed. The mass is also assumed to be concen-

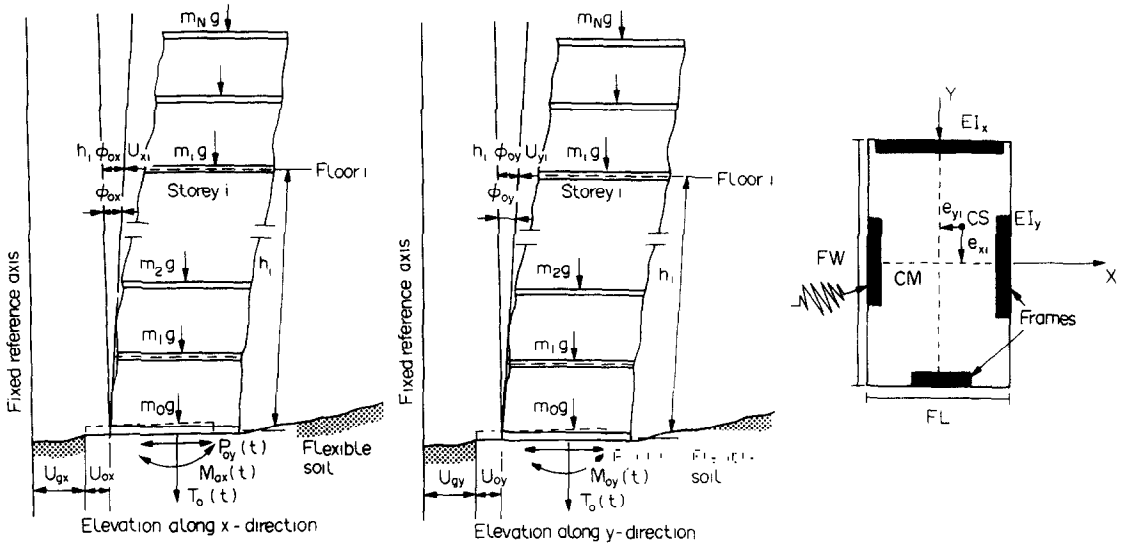


Fig. 1. Idealized three-dimensional asymmetric building–foundation system.

trated at the floor levels. Thus, the centre of mass (CM) is at the geometric centre of the floor plan, and the CM of all the floors lie on one vertical axis, which is generally the case in many multi-storey buildings unless the building has setback.

The floor system is assumed to be rigid compared to the lateral load-resisting system, which may consist of unbraced steel frames. The lateral load-resisting elements are assumed to be arranged parallel to the floor edges thus, they are either along the $X$- or $Y$-directions as shown in Fig. 1. The stiffnesses of the load-resisting elements are such that the system is asymmetric, thus the centre of stiffness (CS) does not coincide with CM. The location of CS may vary from storey to storey, and in this study the CS associated with the storey $i$ is assumed to lie at eccentricities $e_{xi}$ and $e_{yi}$ from CM.

The building–foundation system will be subjected to artificially-generated horizontal free-field ground motions, assumed to be acting at an angle from the $X$-axis ($X$-component acceleration is $\ddot{U}_{gx}$ and the $Y$-component acceleration is $\ddot{U}_{gy}$). Each floor, say floor $i$, has three displacement degrees of freedom, namely, two horizontal displacements $U_{xi}$ and $U_{yi}$ and twist $U_{0i}$. In addition, due to the deformability of foundation the system has five more displacement degrees of freedom, namely, two horizontal translations of the footing ($U_{0x}$ and $U_{0y}$), two rocking rotations of the footing ($\Phi_{0x}$ and $\Phi_{0y}$), and the twist of the footing $U_{0\theta}$. Defining the horizontal translations and the twists, with respect to the vertical axis passing through CM prior to ground motions, the absolute floor displacements and the absolute twist of the CM corresponding to floor $i$ may be given as: along the $X$-direction $= U_{gx} + U_{0x} + h_i\Phi_{0x} + U_{xi}$, along the $Y$-direction $= U_{gy} + U_{0y} + h_i\Phi_{0y} + U_{yi}$, twist $= U_{0\theta} + U_{\theta i}$; where, $h_i$ is the height of floor $i$ from the ground level. Considering the equilibrium of each floor (about the CM), the governing equations of the $N$-floors of the asymmetric superstructure may be developed as

$$\begin{bmatrix}[M] & [0] & [0]\\ [0] & [M] & [0]\\ [0] & [0] & [M]\end{bmatrix}\begin{Bmatrix}\{\ddot{U}_{xi}\}\\ \{r_i\ddot{U}_{0i}\}\\ \{\ddot{U}_{yi}\}\end{Bmatrix} + \begin{bmatrix}[K_{xx}] & [K_{x\theta}] & [0]\\ [K_{x\theta}]^T & [K_{\theta\theta}] & [K_{y\theta}]^T\\ [0] & [K_{y\theta}] & [K_{yy}]\end{bmatrix}\begin{Bmatrix}\{U_{xi}\}\\ \{r_iU_{0i}\}\\ \{U_{yi}\}\end{Bmatrix} = -\begin{bmatrix}[M] & [0] & [0]\\ [0] & [M] & [0]\\ [0] & [0] & [M]\end{bmatrix}\begin{Bmatrix}\{\ddot{U}_{gx} + \ddot{U}_{0x} + h_i\ddot{\Phi}_{ox}\}\\ \{r_i\ddot{U}_{0\theta}\}\\ \{\ddot{U}_{gy} + \ddot{U}_{0y} + h_i\ddot{\Phi}_{oy}\}\end{Bmatrix}. \quad (1)$$

Equation (1) is a $3N \times 3N$ coupled differential equation in terms of ground motions and the footing displacements. In the above equation, and in the equations that follow $\{\alpha_i\}$ is an $N \times 1$ sub-vector of quantity $\alpha_i$, where subscript $i$ denotes that it is associated with floor $i$. $r_i$ is the mass radius of gyration of the $i$th floor deck about the vertical axis through the centre of mass. $[M]$ is the diagonal mass submatrix of order $N \times N$; $[K]$ are the stiffness submatrices of order $N \times N$. The coefficients of the submatrices are given in Appendix A, and they may also be found in [2, 12]. It may be noted that in eqn (1), the second set of equations (equations corresponding to rotational displacement degrees of freedom) have been divided by the corresponding mass radius of gyration ($r_i$). It may also be noted that for symmetric structures, that is when $e_{xi}$ and $e_{yi}$ are zero, the coupling matrices $[K_{x\theta}]$ and $[K_{y\theta}]$ become zero. Equation (1) then reduces to three sets of equations, each corresponding to the $X$-direction, $Y$-direction and the torsional motions of the building. Equation (1) is for undamped systems. The system viscous damping is assumed to be of such a form that the building on rigid foundation admits decomposition

into classical normal modes. Also, assuming that the building–foundation system possesses similar mode shapes as the classical normal modes of the building on rigid foundation, eqn (1) can be uncoupled and written in terms of normal coordinates as

$$\ddot{q}_K + 2\xi_K\omega_K\dot{q}_K + \omega_K^2 q_K = -F_K(t), \quad K = 1\text{-}3N, \quad (2)$$

where, $\omega_K$ and $\xi_K$ are the undamped natural frequency and the damping ratio, respectively, corresponding to the $K$th mode, and $F_K(t) = \alpha_{1K}(\ddot{U}_{gx} + \ddot{U}_{0x}) + \beta_{1K}\ddot{\Phi}_{0x} + \alpha_{2K}r_0\ddot{U}_{00} + \alpha_{3K}(\ddot{U}_{gy} + \ddot{U}_{0y}) + \beta_{3K}\ddot{\Phi}_{0y}$. Here, $r_0$ is the mass radius of gyration of the footing and $\alpha_{1K}$, $\beta_{1K}$, $\alpha_{2K}$, $\alpha_{3K}$, and $\beta_{3K}$ are coefficients corresponding to the $K$th mode, and are given by

$$\alpha_{1K} = \frac{\sum_{i=1}^{N} m_i\gamma_{iK}^x}{\sum_{i=1}^{N} m_i\{\gamma_{iK}^x{}^2\}}, \quad \beta_{1K} = \frac{\sum_{i=1}^{N} m_i h_i\gamma_{iK}^x}{\sum_{i=1}^{n} m_i\{\gamma_{iK}^x{}^2\}},$$

$$\alpha_{2K} = \frac{\sum_{i=1}^{N} m_i\gamma_{iK}^0}{\sum_{i=1}^{N} m_i\{\gamma_{iK}^0{}^2\}}, \quad \alpha_{3K} = \frac{\sum_{i=1}^{N} m_i\gamma_{iK}^y}{\sum_{i=1}^{N} m_i\{\gamma_{iK}^y{}^2\}},$$

$$\beta_{3K} = \frac{\sum_{i=1}^{N} m_i h_i\gamma_{iK}^y}{\sum_{i=1}^{N} m_i\{\gamma_{iK}^y{}^2\}}, \quad K = 1, 2, 3, \ldots, (3N), \quad (2')$$

where $m_i$ is the lumped mass at floor $i$ and $\{\gamma_{iK}^x\}$, $\{\gamma_{iK}^y\}$, and $\{\gamma_{iK}^0\}$ are the sub-vectors of the mode shape corresponding to the $K$th mode of vibration. The structural deformation of each floor may be obtained by the mode superposition relations as

$$\begin{Bmatrix} \{U_{xi}\} \\ \{r_i U_{0i}\} \\ \{U_{yi}\} \end{Bmatrix} = \begin{bmatrix} [\gamma_{iK}^x] \\ [\gamma_{iK}^0] \\ [\gamma_{iK}^y] \end{bmatrix}_{3N\times 3N} \{q_K\}_{3N\times 1}, \quad (3)$$

where $\{q_K\}$ is the array of $3N$ normal coordinates, which may be obtained in terms of ground motions and the footing displacements by solving eqn (2) as

$$q_K = \frac{-1}{\omega_{DK}}\int_0^t F_K(\tau)e^{-\zeta_K\omega_K(t-\tau)}\sin\omega_{DK}(t-\tau)\,d\tau, \quad (4)$$

where $\omega_{DK} = \omega_K\sqrt{(1-\zeta_K^2)}$ is the damped natural frequency. Also note that

$$\ddot{q}_K(t) = \frac{\omega_K}{\sqrt{(1-\zeta_K^2)}}\int_0^t F_K(\tau)e^{-\zeta_K\omega_K(t-\tau)} \times \cos[\omega_{DK}(t-\tau) - \Psi_K]\,d\tau - F_K(t), \quad (4')$$

where $\Psi_K = \tan^{-1}(1-2\zeta_K^2)/(2\zeta_K\sqrt{[1-\zeta_K^2]})$ is the phase angle.

Five more equations are needed in order to completely solve the problem. These equations are developed by considering the equilibrium of the whole system. They are given by

$$m_0(\ddot{U}_{gx} + \ddot{U}_{0x}) + \sum_{i=1}^{N} m_i(\ddot{U}_{gx} + \ddot{U}_{0x} + h_i\ddot{\Phi}_{0x} + \ddot{U}_{xi}) + P_{0x}(t) = 0 \quad (5a)$$

$$m_0(\ddot{U}_{gy} + \ddot{U}_{0y}) + \sum_{i=1}^{N} m_i(\ddot{U}_{gy} + \ddot{U}_{0y} + h_i\ddot{\Phi}_{0y} + \ddot{U}_{yi}) + P_{0y}(t) = 0 \quad (5b)$$

$$I_{tx}\ddot{\Phi}_{0x} + \sum_{i=1}^{N} m_i h_i(\ddot{U}_{gx} + \ddot{U}_{0x} + h_i\ddot{\Phi}_{0x} + \ddot{U}_{xi}) + M_{0x}(t) = 0 \quad (5c)$$

$$I_{ty}\ddot{\Phi}_{0y} + \sum_{i=1}^{N} m_i h_i(\ddot{U}_{gy} + \ddot{U}_{0y} + h_i\ddot{\Phi}_{0y} + \ddot{U}_{yi}) + M_{0y}(t) = 0 \quad (5d)$$

$$m_0 r_0^2\ddot{U}_{00} + \sum_{i=1}^{N} m_i r_i^2(\ddot{U}_{00} + \ddot{U}_{0i}) + T_0(t) = 0, \quad (5e)$$

where $m_0$ and $r_0$ are the mass and the radius of gyration of footing, respectively. $I_{tx}$ and $I_{ty}$ are the total of the mass moment of inertia of the floors and the footing with respect to the $X$ and $Y$ axes. $P_{0x}(t)$, $P_{0y}(t)$, $M_{0x}(t)$, and $M_{0y}(t)$ are the horizontal soil–structure interaction forces and the rocking soil–structure interaction moments in the $X$- and $Y$-directions, respectively. $T_0(t)$ is the torsional soil–structure interaction moment. These soil–structure interactions can be related to footing displacements and are given in the next section. Substitution of floor deformations given by eqn (3), and the corresponding floor accelerations, into eqns (5) result in five integro-differential equations in terms of footing displacements $U_{0x}$, $U_{0y}$, $\Phi_{0x}$, $\Phi_{0y}$, and $U_{00}$

$$m_0(\ddot{U}_{gx} + \ddot{U}_{0x}) + \sum_{K=1}^{3N}\alpha_{1K1}\int_0^t(\ddot{U}_{gx} + \ddot{U}_{0x})\mu_K\,d\tau + \sum_{K=1}^{3N}\beta_{1K1}\int_0^t\ddot{\Phi}_{0x}\mu_K\,d\tau + \sum_{K=1}^{3N}\alpha_{2K1}\int_0^t r_0\ddot{U}_{00}\mu_K\,d\tau + \sum_{K=1}^{3N}\alpha_{3K1}\int_0^t(\ddot{U}_{gy} + \ddot{U}_{0y})\mu_K\,d\tau + \sum_{K=1}^{3N}\beta_{3K1}\int_0^t\ddot{\Phi}_{0y}\mu_K\,d\tau - \left[\sum_{K=1}^{3N}\alpha_{2K1}r_0\ddot{U}_{00} + \sum_{K=1}^{3N}\alpha_{3K1}(\ddot{U}_{gy} + \ddot{U}_{0y}) + \sum_{K=1}^{3N}\beta_{3K1}\ddot{\Phi}_{0y}\right] + P_{0x}(t) = 0 \quad (6a)$$

$$m_0(\ddot{U}_{gy}+\ddot{U}_{0y})+\sum_{K=1}^{3N}\alpha_{1K2}\int_0^t(\ddot{U}_{gx}+\ddot{U}_{0x})\mu_K\,d\tau + \sum_{K=1}^{3N}\beta_{1K2}\int_0^t\ddot{\Phi}_{0x}\mu_K\,d\tau+\sum_{K=1}^{3N}\alpha_{2K2}\int_0^t r_0\ddot{U}_{00}\mu_K\,d\tau + \sum_{K=1}^{3N}\alpha_{3K2}\int_0^t(\ddot{U}_{gy}+\ddot{U}_{0y})\mu_K\,d\tau + \sum_{K=1}^{3N}\beta_{3K2}\int_0^t\ddot{\Phi}_{0y}\mu_K\,d\tau-\left[\sum_{K=1}^{3N}\alpha_{1K2}(\ddot{U}_{gx}+\ddot{U}_{0x}) + \sum_{K=1}^{3N}\beta_{1K2}\ddot{\Phi}_{0x}+\sum_{K=1}^{3N}\alpha_{2K2}r_0\ddot{U}_{00}\right]+P_{0x}(t)=0 \quad (6b)$$

$$I_{tx}\ddot{\Phi}_{0x}+\sum_{K=1}^{3N}\alpha_{1K3}\int_0^t(\ddot{U}_{gx}+\ddot{U}_{0x})\mu_K\,d\tau + \sum_{K=1}^{3N}\beta_{1K3}\int_0^t\ddot{\Phi}_{0x}\mu_K\,d\tau+\sum_{K=1}^{3N}\alpha_{2K3}\int_0^t r_0\ddot{U}_{00}\mu_K\,d\tau + \sum_{K=1}^{3N}\alpha_{3K3}\int_0^t(\ddot{U}_{gy}+\ddot{U}_{0y})\mu_K\,d\tau + \sum_{K=1}^{3N}\beta_{3K3}\int_0^t\ddot{\Phi}_{0y}\mu_K\,d\tau-\left[\sum_{K=1}^{3N}\alpha_{2K3}r_0\ddot{U}_{00} + \sum_{K=1}^{3N}\alpha_{3K3}(\ddot{U}_{gy}+\ddot{U}_{0y})+\beta_{3K3}\ddot{\Phi}_{0y}\right]+M_{0x}(t)=0 \quad (6c)$$

$$I_{ty}\ddot{\Phi}_{0y}+\sum_{K=1}^{3N}\alpha_{1K4}\int_0^t(\ddot{U}_{gx}+\ddot{U}_{0x})\mu_K\,d\tau + \sum_{K=1}^{3N}\beta_{1K4}\int_0^t\ddot{\Phi}_{0x}\mu_K\,d\tau+\sum_{K=1}^{3N}\alpha_{2K4}\int_0^t r_0\ddot{U}_{00}\mu_K\,d\tau + \sum_{K=1}^{3N}\alpha_{3K4}\int_0^t(\ddot{U}_{gy}+\ddot{U}_{0y})\mu_K\,d\tau + \sum_{K=1}^{3N}\beta_{3K4}\int_0^t\ddot{\Phi}_{0y}\mu_K\,d\tau-\left[\sum_{K=1}^{3N}\alpha_{1K4}(\ddot{U}_{gx}+\ddot{U}_{0x}) + \sum_{K=1}^{3N}\beta_{1K4}\ddot{\Phi}_{0x}+\sum_{K=1}^{3N}\alpha_{2K4}r_0\ddot{U}_{00}\right]+M_{0y}(t)=0 \quad (6d)$$

$$\left[m_0r_0^2+\sum_{i=1}^{N}m_ir_i^2\right]\ddot{U}_{00} + \sum_{K=1}^{3N}\alpha_{1K5}\int_0^t(\ddot{U}_{gx}+\ddot{U}_{0x})\mu_K\,d\tau + \sum_{K=1}^{3N}\beta_{1K5}\int_0^t\ddot{\Phi}_{0x}\mu_K\,d\tau+\sum_{K=1}^{3N}\alpha_{2K5}\int_0^t r_0\ddot{U}_{00}\mu_K\,d\tau + \sum_{K=1}^{3N}\alpha_{3K5}\int_0^t(\ddot{U}_{gy}+\ddot{U}_{0y})\mu_K\,d\tau + \sum_{K=1}^{3N}\beta_{3K5}\int_0^t\ddot{\Phi}_{0y}\mu_K\,d\tau-\left[\sum_{K=1}^{3N}\alpha_{1K5}(\ddot{U}_{gx}+\ddot{U}_{0x}) + \sum_{K=1}^{3N}\beta_{1K5}\ddot{\Phi}_{0x}+\sum_{K=1}^{3N}\alpha_{2K5}r_0\ddot{U}_{00} + \sum_{K=1}^{3N}\alpha_{3K5}(\ddot{U}_{gy}+\ddot{U}_{0y})+\sum_{K=1}^{3N}\beta_{3K5}\ddot{\Phi}_{0y}\right]+T_0(t)=0, \quad (6e)$$

where

$$\mu_K(\tau)=\frac{\omega_K}{\sqrt{(1-\zeta_K^2)}}e^{-\zeta_K\omega_K(t-\tau)} \times\cos[\omega_{DK}(t-\tau)-\Psi_K]$$

and the other coefficients in eqns (6) are

$$\alpha_{1K1}=\alpha_{1K}\sum_{i=1}^{N}m_i\gamma_{iK}^x,\quad \alpha_{1K2}=\alpha_{1K}\sum_{i=1}^{N}m_i\gamma_{iK}^y,$$

$$\alpha_{1K3}=\alpha_{1K}\sum_{i=1}^{N}m_ih_i\gamma_{iK}^x,\quad \alpha_{1K4}=\alpha_{1K}\sum_{i=1}^{N}m_ih_i\gamma_{iK}^y,$$

$$\alpha_{1K5}=\alpha_{1K}\sum_{i=1}^{N}m_ir_i\gamma_{iK}^\theta,\quad K=1,2,3,\ldots,3N. \quad (7)$$

Expressions for $\beta_{1K1}$, $\alpha_{2K1}$, $\alpha_{3K1}$, $\beta_{3K1}$, etc. can be obtained from eqn (7) by replacing $\alpha_{1K}$ by $\beta_{1K}$, $\alpha_{2K}$, $\alpha_{3K}$, $\beta_{3K}$, respectively.

*Dynamic soil–structure interactions*

As indicated previously, $P_{0x}(t)$, $P_{0y}(t)$, $M_{0x}(t)$, $M_{0y}(t)$, and $T_0(t)$ are the dynamic loads imposed by the structure on the foundation, and vice versa. These loads can be related to footing displacements $U_{0x}$, $U_{0y}$, $\Phi_{0x}$, $\Phi_{0y}$ and $U_{00}$. In general, the dynamic soil–structure interaction force–displacement relationships depend on the frequency of excitation, thus, they are usually developed in the frequency domain. A frequency domain analysis first requires a Fourier transformation of governing equations of the building–foundation system into the frequency domain. Then the response of the system at various excitation frequencies is determined. Response to an arbitrary ground motion is then determined by considering the range of frequencies over which the ground motion and building–foundation system have significant components, and then performing a Fourier synthesis of the frequency response to obtain the responses in the time domain. Such a procedure, often referred to as the direct method, requires a large computational effort, particularly for structures with many degrees of freedom such as three-dimensional asymmetric multi-storey buildings. In consideration of this difficulty various frequency independent, but approximate, dynamic soil–structure interaction relationships have been proposed in the literature [13–15].

In this study the soil–structure interaction force–displacement relationships proposed by Veletsos and Verbic [13] and Veletsos and Nair [14] have been used. These relationships, in general, depend on

the Poisson's ratio ($\nu$) of the foundation material. For a Poisson's ratio of $\nu = 0.45$, which may be considered as a representative value for soil, these relationships are as below [13, 14]

$$P_{0x}(t) = K_{Ux}\left[U_{0x}(t) + 0.6\left(\frac{r}{c_s}\right)\dot{U}_{0x}(t)\right] \quad (8a)$$

$$P_{0y}(t) = K_{Uy}\left[U_{0y}(t) + 0.6\left(\frac{r}{c_s}\right)\dot{U}_{0y}(t)\right] \quad (8b)$$

$$M_{0x}(t) = K_{\Phi x}\left[0.55\Phi_{0x}(t) + 0.36\left(\frac{r}{c_s}\right)\dot{\Phi}_{0x}(t) + 0.023\left(\frac{r}{c_s}\right)^2\ddot{\Phi}_{0x} + 0.563\left(\frac{c_s}{r}\right) \times \left\{\int_0^t \Phi_{0x}(\tau)e^{-1.25(c_s/r)(t-\tau)}\,d\tau\right\}\right] \quad (8c)$$

$$M_{0y}(t) = K_{\Phi y}\left[0.55\Phi_{0y}(t) + 0.36\left(\frac{r}{c_s}\right)\dot{\Phi}_{0y}(t) + 0.023\left(\frac{r}{c_s}\right)^2\ddot{\Phi}_{0y} + 0.563\left(\frac{c_s}{r}\right) \times \left\{\int_0^t \Phi_{0y}(\tau)e^{-1.25(c_s/r)(t-\tau)}\,d\tau\right\}\right] \quad (8d)$$

$$T_0(t) = K_{U\theta}\left[0.575U_{0\theta}(t) + 0.292\left(\frac{r}{c_s}\right)\dot{U}_{0\theta}(t) + 0.619\left(\frac{c_s}{r}\right)\left\{\int_0^t U_{0\theta}(\tau)e^{-1.456(c_s/r)(t-\tau)}\,d\tau\right\}\right], \quad (8e)$$

where the static-stiffness coefficients are given by

$$K_{Ux} = K_{Uy} = \frac{8Gr}{2-\nu}, \quad K_{\Phi x} = K_{\Phi y} = \frac{8Gr^3}{3(1-\nu)}, \quad K_{U\theta} = \frac{16Gr^3}{3} \quad (8f)$$

and where $c_s$ is the shear wave velocity of the foundation half-space, $\nu$ is the Poisson's ratio of the foundation material, $G$ is the shear modulus of elasticity of the foundation soil, which may be related as $G = c_s^2\rho$, where $\rho$ is the mass density of the foundation material, and $r$ is the equivalent radius of the rigid circular foundation. The original soil–structure interaction relationships as presented in [13, 14] are for a rigid circular disc footing on elastic half-space. However, limited results that have been obtained for rectangular footing indicate that they are similar to those for circular footing of the same plan area [16]. In this study, the time domain integro-differential relationships for a circular footing given by eqns (8) have been used, with $r$ taken as the radius of a circle having the same plan area of the rectangular rigid footing of the building. For soil having a different Poisson's ratio, the form of the dynamic force–displacement relationships are the same, however, the numerical constants in the relationships would be different.

*Numerical step-by-step time-history analysis*

Equations (6) and (8), which are coupled integro-differential equations in terms of footing displacements, are now the governing equations for the behaviour of asymmetric building–foundation system. These equations are solved in this study using a numerical step-by-step time-history analysis. Without going through the mathematical details, in what follows, first the integrations and the differentials involved in these equations have been replaced by displacements only, using the Trapezoidal rule and Newmark's constant-average-acceleration algorithms [11]. Assigning the terms associated with the current time step to the left-hand side and the values associated with the previous time steps to the right-hand side, the governing equations have been reduced to the following system of linear equations

$$\begin{bmatrix} A_{11} & A_{12} & A_{13} & A_{14} & A_{15} \\ A_{21} & A_{22} & A_{23} & A_{24} & A_{25} \\ A_{31} & A_{32} & A_{33} & A_{34} & A_{35} \\ A_{41} & A_{42} & A_{43} & A_{44} & A_{45} \\ A_{51} & A_{52} & A_{53} & A_{54} & A_{55} \end{bmatrix} \begin{Bmatrix} U_{0x}(t) \\ U_{0y}(t) \\ \Phi_{0x}(t) \\ \Phi_{0y}(t) \\ r_0 U_{0\theta}(t) \end{Bmatrix} = \begin{Bmatrix} B_1 \\ B_2 \\ B_3 \\ B_4 \\ B_5 \end{Bmatrix}. \quad (9)$$

The expressions for the coefficients $A_{ij}$ and $B_i$ are given in Appendix B. It may be noted that $A_{ij}$ are constants at each time step, whereas $B_i$ requires summation of quantities associated with time 0 to $t - \Delta t$. Thus, the calculation of $B_i$ requires considerable computational effort, which has been greatly improved by the use of recurrence formulae [10, 11]. The solution for eqn (9) gives the footing displacements at each time step, from which footing accelerations at each time step may be established. The structural deformations, storey shears and storey torque may be obtained by back-substitution of footing accelerations into eqns (4) and (3). Thus, in the method of analysis for the seismic response of three-dimensional asymmetric building–foundation system presented in this paper, the governing equations of the whole system with $3N + 5$ degrees of freedom are reduced to five coupled linear equations. This reduction in degrees of freedom allows a considerable saving in computing time. It has been shown that the seismic response of a system having classical normal modes can be accurately obtained by considering only the first few modes [2]. It has also been shown that this phenomenon also exists in building–foundation systems, which do not possess classical normal modes [8, 10, 11]. Thus, an additional saving in computing time can be achieved by

considering only the first few modes of vibration in the summations involved in eqns (6).

## NUMERICAL ANALYSIS AND DISCUSSIONS

In order to illustrate the application of the above-developed method of analysis and to obtain the soil–structure interaction effects on a three-dimensional asymmetric multi-storey building, the configuration of the building shown in Fig. 1 was considered. The building was 10 storeys high. All storeys were of the same height of 150 in. The building consists of four unbraced steel frames joined at each floor level by a rigid diaphragm. The total flexural rigidities of these frames were taken to be: along the $X$-direction $\Sigma EI_x = 1260 \times 10^9$ lbf in$^2$ from floors 1 to 5, and $\Sigma EI_x = 720 \times 10^9$ lbf in$^2$ from floors 6 to 10; along the $Y$-direction $\Sigma EI_y = 900 \times 10^9$ lbf in$^2$ from floors 1 to 5, and $\Sigma EI_y = 450 \times 10^9$ lbf in$^2$ from floors 6 to 10. Stiffness asymmetry was generated by dividing the above-indicated flexural rigidities unequally among the two frames. If the flexural rigidities of the two frames in any given direction were the same, then the building becomes symmetric in that direction. In this study, the eccentricities of all the stories were assumed to be the same, and the values of the eccentricities ranged between 0.0 and 0.20 times the building dimensions. All floors, including the footing, were assumed to be identical with length of the building $FL = 400$ in. and the width of the building $FW = 800$ in. The masses at all the floor levels were the same ($m = 0.725$ psi). The mass of the footing was taken to be $m_0 = 1.45$ psi. The natural periods of the superstructure on rigid foundation, including the torsional modes, ranged between 0.625 and 0.025 sec. The damping ratio of the superstructure in each mode of vibration was taken as 5%.

Recall that the dynamic soil–structure interaction relationships given by eqns (8) were developed for a massless rigid circular disc. In this study, however, they have been applied to a rectangular footing with mass in an approximate manner by the use of an equivalent radius, where $r$ was taken as the radius of circle having the same plan area of the rectangular rigid footing of the building. The foundation soil was assumed to be clay ($\rho = 80$ lb/ft$^3$, $\nu = 0.45$), and in order to study the effects of soil–structure interaction the shear wave velocity of the half-space material was selected to be between 333 ft/sec (soft) and 3333 ft/sec (rigid). The responses of the asymmetric building–foundation system were established when it was subjected to an artificially-generated accelerogram having a peak acceleration of 0.35 $g$. The duration of the accelerogram was 20 sec. This accelerogram was artificially-generated such that its spectrum agrees with the Newmark–Hall design spectrum. A comparison of the generated spectrum with the Newmark–Hall design spectrum indicated an excellent agreement [12]. Since, the study involves a three-dimensional asymmetric building–foundation system subjected to bi-directional earthquake excitation, here, the artificial accelerogram was applied at 30° to the $X$-direction. Thus, in the analysis $\ddot{U}_{gx} = \ddot{U}_g \cos 30°$ and $\ddot{U}_{gy} = \ddot{U}_g \sin 30°$, where $\ddot{U}_g$ are the artificially-generated accelerations.

### *Effects of time step and the number of normal mode shapes*

The value of the time step $\Delta t$ used in the numerical step-by-step time-history analysis can influence the convergence and the accuracy of the results. Therefore, the effects of time step on the response of a three-dimensional asymmetric building–foundation system were established by considering the time steps $\Delta t = 0.002$, 0.004, 0.005, 0.01, and 0.02 sec. The response quantities, namely, maximum $X$-component, and $Y$-component floor displacements, maximum floor twist, maximum $X$-component, and $Y$-component storey shears, maximum floor torque were chosen for the study. Based on these results, which are not shown here, but are given in [12], it was concluded that the time step $\Delta t = 0.02$ sec is sufficiently small to produce converged and accurate results. Thus, in the subsequent calculations and in the results presented in this paper a time step of $\Delta t = 0.02$ sec was used.

It was indicated in the previous section that accurate results may be obtained by considering only the first few normal modes of vibration. The effects of the number of modes on the response of the asymmetric building–foundation system were established by considering the first 1, 3, 5, 10, and 30 normal mode shapes. These results (again not shown in the paper but are given in [12]) indicate that the first 10 modes of vibration give sufficiently accurate floor displacements and forces. Thus, the results shown in this paper are based on the first 10 normal modes of vibration.

### *Results*

Figures 2 and 3 show the envelopes of the responses of the building–foundation system under consideration subjected to artificially generated acceleration described above. Envelopes indicate the maximum values of the responses that have occurred during the whole excitation. Figure 2 shows the effects of shear wave velocity (constant $e_{xi} = 0.1\ FW$, $e_{yi} = 0.1$ FL) on the maximum responses of the system, whereas Fig. 3 shows the effect of eccentricity (constant shear wave velocity $c_s = 333$ ft/sec) on the responses of the system. In these figures, the floor deflections, and twists indicate the absolute displacements of the CM with respect to the ground, thus they include the footing displacements. The displacements corresponding to floor level 0 show the footing displacements. Considerable footing displacements are induced, particularly when the foundation soil is very soft (i.e. $c_s = 333$ ft/sec). The maximum values of the footing displacements observed in these analyses were $U_{0x} = 0.23$ in.,

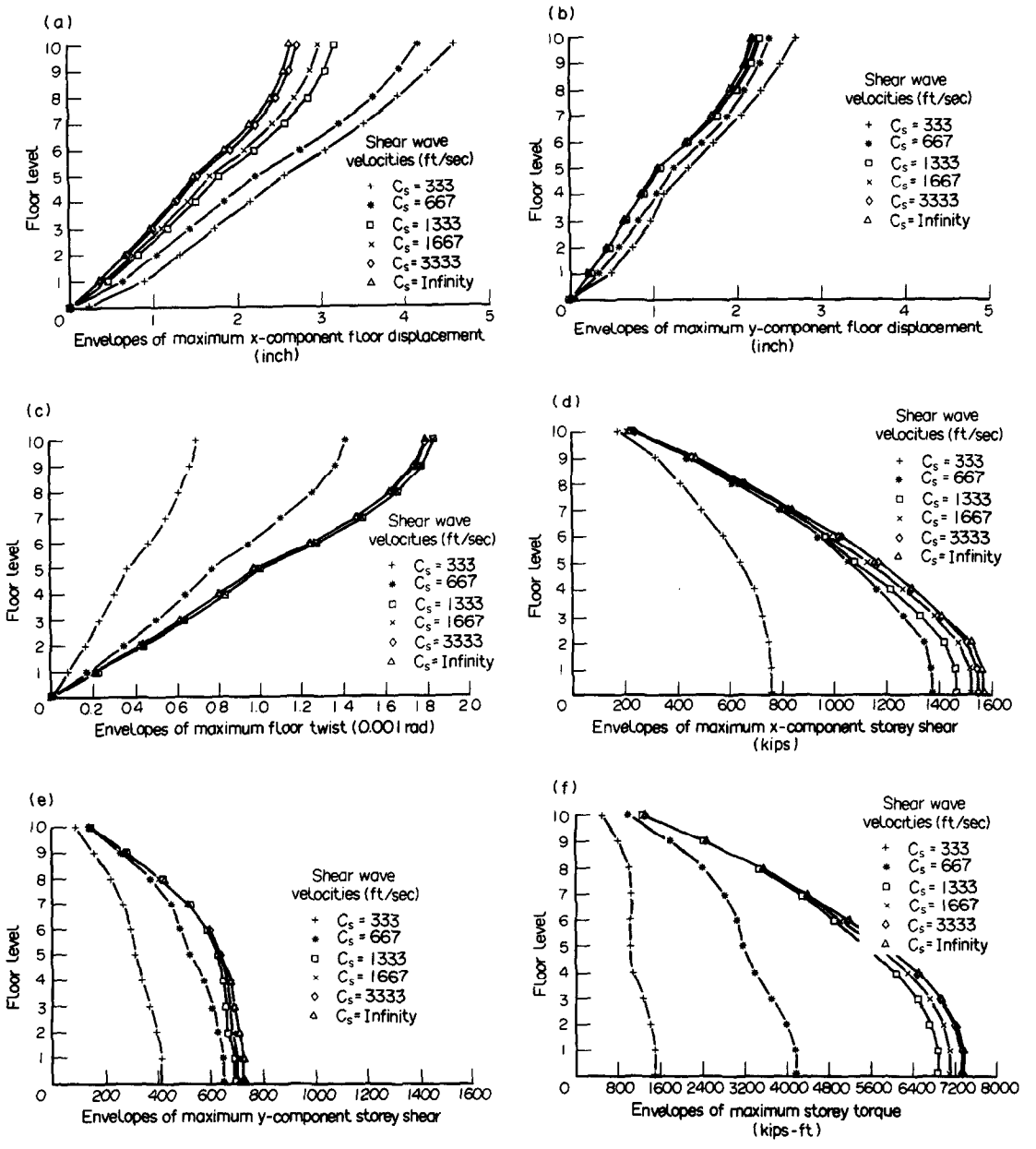


Fig. 2. (a) Effects of soil–structure interaction on the envelopes of maximum $x$-component floor displacement of a 10-storey building subjected to artificially-generated accelerogram ($e_x = 80$ in., $e_y = 40$ in., time step = 0.02 sec, number of normal mode shapes = 10). (b) Effects of soil–structure interaction on the envelopes of maximum $y$-component floor displacement of a 10-storey building subjected to artificially-generated accelerogram ($e_x = 80$ in., $e_y = 40$ in., time step = 0.02 sec, number of normal mode shapes = 10). (c) Effects of soil–structure interaction on the envelopes of maximum floor twist of a 10-storey building subjected to artificially-generated accelerogram ($e_x = 80$ in., $e_y = 40$ in., time step = 0.02 sec, number of normal mode shapes = 10). (d) Effects of soil–structure interaction on the envelopes of maximum $x$-component storey shear of a 10-storey building subjected to artificially-generated accelerogram ($e_x = 80$ in., $e_y = 40$ in., time step = 0.02 sec, number of normal mode shapes = 10). (e) Effects of soil–structure interaction on the envelopes of maximum $y$-component storey shear of a 10-storey building subjected to artificially-generated accelerogram ($e_x = 80$ in., $e_y = 40$ in., time step = 0.02 sec, number of normal mode shapes = 10). (f) Effects of soil–structure interaction on the envelopes of maximum storey torque of a 10-storey building subjected to artificially-generated accelerogram ($e_x = 80$ in., $e_y = 40$ in., time step = 0.02 sec, number of normal mode shapes = 10).

$U_{0y} = 0.13$ in., $\Phi_{0x} = 0.0017$ rad, $\Phi_{0y} = 0.0009$ rad, and $U_{0\theta} = 0.00000017$ rad. It may be noted that the foundation soil significantly influences the footing displacements, however, the eccentricity does not appear to alter the amount of footing displacements.

The effects of deformability of the foundation may be studied from Fig. 2, where the results corresponding to rigid foundation ($c_s$ = infinity) provide the basis for comparison. Figures 2(a) and (b) show the envelopes of the $X$- and $Y$-components displace-

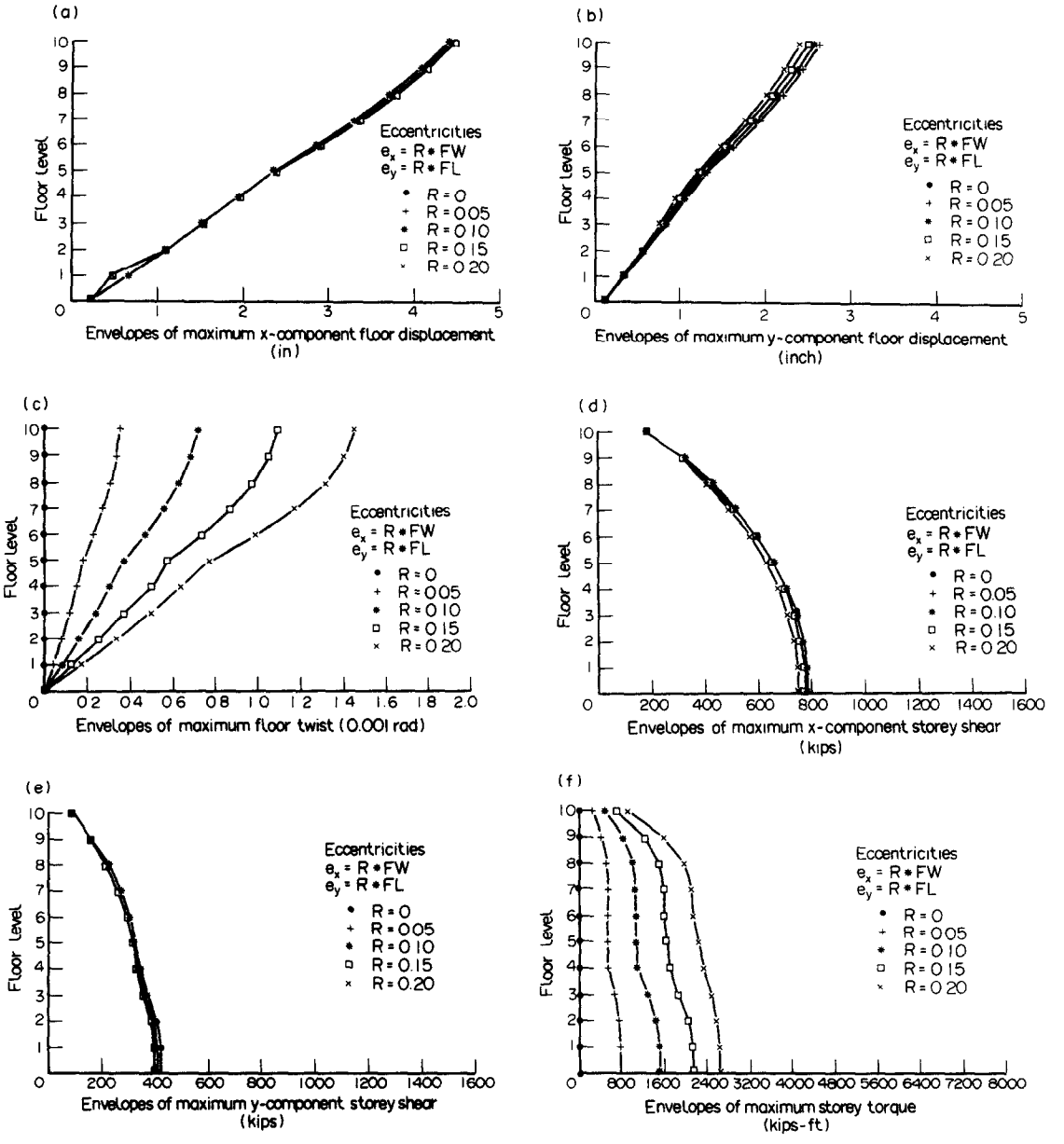


Fig. 3. (a) Effects of eccentricity on the envelopes of maximum $x$-component floor displacement of a 10-storey building subjected to artificially-generated accelerogram ($C_s$ = 333 ft/sec, time step = 0.02 sec, number of normal mode shapes = 10). (b) Effects of eccentricity on the envelopes of maximum $y$-component storey floor displacement of a 10-storey building subjected to artificially-generated accelerogram ($C_s$ = 333 ft/sec, time step = 0.02 sec, number of normal mode shapes = 10). (c) Effects of eccentricity on the envelopes of maximum floor twist of a 10-storey building subjected to artificially-generated accelerogram ($C_s$ = 333 ft/sec, time step = 0.02 sec, number of normal mode shapes = 10). (d) Effects of eccentricity on the envelopes of maximum $x$-component storey shear of a 10-storey building subjected to artificially-generated accelerogram ($C_s$ = 333 ft/sec, time step = 0.02 sec, number of normal mode shapes = 10). (e) Effects of eccentricity on the envelopes of maximum $y$-component storey shear of a 10-storey building subjected to artificially-generated accelerogram ($C_s$ = 333 ft/sec, time step = 0.02 sec, number of normal mode shapes = 10). (f) Effects of eccentricity on the envelopes of maximum floor torque of a 10-storey building subjected to artificially-generated accelerogram ($C_s$ = 333 ft/sec, time step = 0.02 sec, number of normal mode shapes = 10).

ments of the CM, respectively. The building experiences larger $X$-component displacements compared to $Y$-component displacements, which may be due to the fact that a larger component of the ground acceleration was applied along the $X$-direction. From these figures it is evident that the foundation flexibility results in a substantially increased lateral deflection. For example, the roof $X$-component deflections of the building founded on soil with $c_s$ = 333 ft/sec are increased by 170%. Figure 2(c) shows the twists of the floors about the axis passing through CM. The soft soil conditions reduce the amount of twists

induced in an asymmetric building. Figures 2(d)–(f) show the $X$-component storey shear, $Y$-component storey shear, and the storey torque, respectively. From these figures it is clear that the soft soil conditions reduce the shear and torque exerted on the building. It may be noticed that when the building is founded on soil with $c_s = 333$ ft/sec, the storey shears have been reduced by 50%, and the storey torques have been reduced to almost 20% of what would have been induced, if the building had been on a rigid foundation. From these figures it may be stated that, soft soil conditions do influence the responses of asymmetric buildings, particularly when $c_s$ is lower than, for example 1000 ft/sec. Although, the lateral deflections were increased, the twists, storey shears, and torques were decreased considerably indicating a beneficial effect due to soft soil conditions.

The effects of eccentricity may be studied from Fig. 3, where the results corresponding to symmetric buildings ($R = 0$) provide the basis for comparison. From Figs 3(a) and (b), it appears that the eccentricities do not change the maximum lateral deflections of the buildings which have been taken at CM. However, from Fig. 3(c), it is clear that the eccentricities do significantly increase the floor twists. Note, in this figure that the floor twists are zero when the building is symmetric, however, when eccentricities were increased from $R = 0.05$ to $R = 0.2$, the twists were also increased by four times. As one would have expected, Figs 3(d) and (e) show that the total storey shears taken at CM remain the same for increasing eccentricities. However, as shown in Fig. 3(f), significant storey torques are induced when the buildings are asymmetric. From these figures, it may be stated that although the maximum lateral deflections and the lateral shears induced by the eccentricities are not significant, considerable twists and torques are induced, indicating that the deflections and the shears in the frames farther away from the CM will be considerably increased due to increasing eccentricities.

## CONCLUSIONS

This paper provides a method of analysis to determine the seismic responses of three-dimensional asymmetric building–foundation systems. In this method of analysis the computational efficiency has been greatly increased by: (a) the reduction of $3N + 5$ governing equations to five coupled integro-differential equations; (b) the use of recurrence formulae to evaluate the convolution integrals; and (c) considering only the first few normal modes of vibration in the computations. A numerical example was shown to illustrate the application of the method of analysis developed in this paper, and to obtain the effects of soil–structure interaction and eccentricity. The results indicate that the soft soil conditions do influence the response of asymmetric buildings, particularly when the shear wave velocity of the foundation is lower than, say, 1000 ft/sec. When the foundation soil is soft, the lateral deflections were increased, but the twists, storey shears, and torques were decreased considerably indicating a beneficial effect due to soft soil conditions. Increasing asymmetry does not alter the maximum lateral deflections of the CM, and the total lateral shears induced in the building. However, increasing asymmetry induces larger twists and storey torques, resulting in higher deflections and shears, particularly at the frames farther away from the CM.

*Acknowledgements*—The support of the Natural Sciences and Engineering Research Council of Canada and of the Asian Institute of Technology is gratefully acknowledged.

## REFERENCES

1. J. Gluck, Lateral-load analysis of asymmetric multistory structures. *ASCE J. Struct. Div.* **96**, 317–333 (1970).
2. C. L. Kan and A. K. Chopra, Elastic earthquake analysis of torsionally coupled multistorey buildings. *Earthquake Engng Struct. Dynamics* **5**, 395–412 (1977).
3. Y. Bozorgnia and W. K. Tso, Inelastic earthquake response of asymmetric structures. *ASCE J. Struct. Engng* **112**, 383–400 (1986).
4. A. M. Chandler and G. L. Hutchinson, Torsional coupling effects in earthquake response of asymmetric buildings. *Engng Struct.* **8**, 222–236 (1986).
5. M. R. Maheri, A. M. Chandler and R. H. Bassett, Coupled lateral-torsional behaviour of frame structures under earthquake loading. *Earthquake Engng Struct. Dynamics* **20**, 61–85 (1991).
6. R. A. Parmelee, D. S. Perelman and S. L. Lee, Seismic response of multiple-story structures on flexible foundations. *Bull. Seismol. Soc. Amer.* **59**, 1061–1070 (1969).
7. A. K. Chopra and J. A. Gutierrez, Earthquake response analysis of multistorey buildings including foundation interaction. *Earthquake Engng Struct. Dynamics* **3**, 65–77 (1974).
8. P. Karasudhi, T. Balendra and S. L. Lee, An efficient method of seismic analysis of structure–foundation systems. *Geotechnical Engng* **6**, 133–154 (1975).
9. Y. K. Lin and W. F. Wu, A closed form earthquake response analysis of multistorey building on compliant soil. *J. Struct. Mech.* **12**, 87–110 (1984).
10. K. S. Sivakumaran and T. Balendra, Seismic response of multistorey buildings including foundation interaction and $P - \Delta$ effects. *Engng Structures* **9**, 277–284 (1987).
11. K. S. Sivakumaran, Seismic analysis of monosymmetric multistorey buildings including foundation interaction. *J. Comput. Struct.* **36**, 99–107 (1990).
12. Min-Shay Lin, Seismic response of asymmetric multistorey buildings. M.Eng. thesis, Asian Institute of Technology, Bangkok (1991).
13. A. S. Veletsos and B. Verbic, Basic response functions for elastic foundations. *ASCE J. Engng Mech.* **100**, 189–201 (1974).
14. A. S. Veletsos and V. V. D. Nair, Torsional vibration of viscoelastic foundations. *ASCE J. Geotechnical Engng Div.* **100**, 225–246 (1974).
15. J. P. Wolf and D. R. Somaini, Approximate dynamic model of embedded foundation in time domain. *Earthquake Engng Struct. Dynamics* **14**, 683–703 (1986).
16. W. T. Thomson and T. Kobori, Dynamic compliance of rectangular foundations on an elastic half-space. *J. Appl. Mech.* **30**, 579–584 (1963).

## APPENDIX A

*The mass submatrix* [M]

$$[M] = \begin{bmatrix} m_1 & & & & & \\ & m_2 & & & 0 & \\ & & \ddots & & & \\ & & & m_i & & \\ & 0 & & & \ddots & \\ & & & & & m_{N-1} \\ & & & & & & m_N \end{bmatrix}, \tag{A.1}$$

where $m_i$ is the lumped mass at floor $i$.

*The stiffness sub-matrices*

$$[K_{xx}] = \begin{bmatrix} K_{x1}+K_{x2} & -K_{x2} & & & & & \\ -K_{x2} & K_{x2}+K_{x3} & -K_{x3} & & 0 & & \\ & \ddots & \ddots & \ddots & & & \\ & & -K_{xi} & K_{xi}+K_{x(i+1)} & -K_{x(i+1)} & & \\ & & & \ddots & \ddots & \ddots & \\ & 0 & & & & -K_{xN} & \\ & & & & & -K_{xN} & K_{xN} \end{bmatrix}, \tag{A.2}$$

$$[K_{yy}] = \begin{bmatrix} K_{y1}+K_{y2} & -K_{y2} & & & & & \\ -K_{y2} & K_{y2}+K_{y3} & -K_{y3} & & 0 & & \\ & \ddots & \ddots & \ddots & & & \\ & & -K_{yi} & K_{yi}+K_{y(i+1)} & -K_{y(i+1)} & & \\ & & & \ddots & \ddots & \ddots & \\ & 0 & & & & -K_{yN} & \\ & & & & & -K_{yN} & K_{yN} \end{bmatrix}, \tag{A.3}$$

where $K_{xi} = \Sigma k_{jxi}$ and $K_{yi} = \Sigma k_{jyi}$ are the total translational stiffnesses of the $i$th story in $X$- and $Y$-directions, respectively. $k_{jxi}$ and $k_{jyi}$ represent the translational stiffnesses of the $j$th load resisting element at storey $i$ along the $X$- and $Y$-directions, respectively

$$[K_{\theta\theta}] = \begin{bmatrix} \frac{K_{\theta1}+K_{\theta2}}{r_1^2} & \frac{-K_{\theta2}}{r_1 r_2} & & & & & \\ \frac{-K_{\theta2}}{r_2 r_1} & \frac{K_{\theta2}+K_{\theta3}}{r_2^2} & \frac{-K_{\theta3}}{r_2 r_3} & & 0 & & \\ & \ddots & \ddots & \ddots & & & \\ & & \frac{-K_{\theta i}}{r_i r_{(i-1)}} & \frac{K_{\theta i}+K_{\theta(i+1)}}{r_i^2} & \frac{-K_{\theta(i+1)}}{r_i r_{(i+1)}} & & \\ & & & \ddots & \ddots & \ddots & \\ & 0 & & & & \frac{-K_{\theta N}}{r_{(N-1)} r_N} & \\ & & & & & \frac{-K_{\theta N}}{r_N r_{(N-1)}} & \frac{K_{\theta N}}{r_N^2} \end{bmatrix}, \tag{A.4}$$

where $K_{\theta i} = \Sigma k_{jxi} y_i^2 + \Sigma k_{jyi} x_i^2 + \Sigma k_{j\theta i}$, and where $(x_j, y_j)$ is the coordinate of the $j$th element with respect to $X$ and $Y$ axis. The rotational stiffness of the $j$th load resisting element at storey $i$ may be defined as $k_{j\theta i}$

$$[K_{x\theta}] =$$

$$\begin{bmatrix}
-\dfrac{e_{x1}K_{x1}+e_{x2}K_{x2}}{r_1} & \dfrac{e_{x2}K_{x2}}{r_2} & & & & & \\
\dfrac{e_{x2}K_{x2}}{r_1} & -\dfrac{e_{x2}K_{x2}+e_{x3}K_{x3}}{r_2} & \dfrac{e_{x3}K_{x3}}{r_3} & & 0 & & \\
 & \ddots & \ddots & \ddots & & & \\
 & & \dfrac{e_{xi}K_{xi}}{r_{(i-1)}} & -\dfrac{e_{xi}K_{xi}+e_{x(i+1)}K_{x(i+1)}}{r_i} & \dfrac{e_{x(i+1)}K_{x(i+1)}}{r_{(i+1)}} & & \\
 & & & \ddots & \ddots & \ddots & \\
 & 0 & & & \dfrac{e_{xN}K_{xN}}{r_{(N-1)}} & -\dfrac{e_{xN}K_{xN}}{r_N} & \dfrac{e_{xN}K_{xN}}{r_N}
\end{bmatrix}, \tag{A.5}$$

$$[K_{y\theta}] =$$

$$\begin{bmatrix}
\dfrac{e_{y1}K_{y1}+e_{y2}K_{y2}}{r_1} & -\dfrac{e_{y2}K_{y2}}{r_2} & & & & & \\
-\dfrac{e_{y2}K_{y2}}{r_1} & \dfrac{e_{y2}K_{y2}+e_{y3}K_{y3}}{r_2} & -\dfrac{e_{y3}K_{y3}}{r_3} & & 0 & & \\
 & \ddots & \ddots & \ddots & & & \\
 & & -\dfrac{e_{yi}K_{yi}}{r_{(i-1)}} & \dfrac{e_{yi}K_{yi}+e_{y(i+1)}K_{y(i+1)}}{r_i} & -\dfrac{e_{y(i+1)}K_{y(i+1)}}{r_{i+1}} & & \\
 & & & \ddots & \ddots & \ddots & \\
 & 0 & & & -\dfrac{e_{yN}K_{yN}}{r_{(N-1)}} & \dfrac{e_{yN}K_{yN}}{r_N} & \dfrac{e_{yN}K_{yN}}{r_N}
\end{bmatrix}. \tag{A.6}$$

The storey eccentricities may be calculated from the stiffness and the location of the load resisting elements as

$$e_{xi} = \frac{\sum k_{jyi} x_j}{K_{yi}}, \quad e_{yi} = \frac{\sum k_{jxi} y_j}{K_{xi}} \tag{A.7}$$

## APPENDIX B

*The coefficients of* $A_{ij}$ *and* $B_j$

$$A_{11} = \frac{4}{\Delta t^2} m_0 + \frac{2}{\Delta t} \sum_{K=1}^{3N} \alpha_{1k1} \mu_K(0) + K_{Ux}\left[1 + \frac{2}{\Delta t} 0.6\left(\frac{r}{c_s}\right)\right]$$

$$A_{12} = \sum_{K=1}^{3N} \alpha_{3K1}\left[\frac{2}{\Delta t}\mu_K(0) - \frac{4}{\Delta t^2}\right]$$

$$A_{13} = \frac{2}{\Delta t} \sum_{K=1}^{3N} \beta_{1K1} \mu_K(0)$$

$$A_{14} = \sum_{K=1}^{3N} \beta_{3K1}\left[\frac{2}{\Delta t}\mu_K(0) - \frac{4}{\Delta t^2}\right]$$

$$A_{15} = \sum_{K=1}^{3N} \alpha_{2K1}\left[\frac{2}{\Delta t}\mu_K(0) - \frac{4}{\Delta t^2}\right]$$

$$A_{21} = \sum_{K=1}^{3N} \alpha_{1K2}\left[\frac{2}{\Delta t}\mu_K(0) - \frac{4}{\Delta t^2}\right]$$

$$A_{22} = \frac{4}{\Delta t^2} m_0 + \frac{2}{\Delta t} \sum_{K=1}^{3N} \alpha_{3K2} \mu_K(0) + K_{Uy}\left[1 + \frac{2}{\Delta t} 0.6\left(\frac{r}{c_s}\right)\right]$$

$$A_{23} = \sum_{K=1}^{3N} \beta_{1K2}\left[\frac{2}{\Delta t}\mu_K(0) - \frac{4}{\Delta t^2}\right]$$

$$A_{24} = \frac{2}{\Delta t}\sum_{K=1}^{3N} \beta_{3K2}\mu_K(0)$$

$$A_{25} = \sum_{K=1}^{3N} \alpha_{2K2}\left[\frac{2}{\Delta t}\mu_K(0) - \frac{4}{\Delta t^2}\right]$$

$$A_{31} = \frac{2}{\Delta t}\sum_{K=1}^{3N} \alpha_{1K3}\mu_K(0)$$

$$A_{32} = \sum_{K=1}^{3N} \alpha_{3K3}\left[\frac{2}{\Delta t}\mu_K(0) - \frac{4}{\Delta t^2}\right]$$

$$A_{33} = \frac{4}{\Delta t^2} I_{tx} + \frac{2}{\Delta t}\sum_{k=1}^{3N} \beta_{1K3}\mu_K(0) + K_{\phi x}\left[0.55 + \frac{2}{\Delta t}0.36\left(\frac{r}{c_s}\right) + \frac{4}{\Delta t^2}0.023\left(\frac{r}{c_s}\right)^2 + \frac{\Delta t}{2}0.563\left(\frac{c_s}{r}\right)\right]$$

$$A_{34} = \sum_{K=1}^{3N} \beta_{3K3}\left[\frac{2}{\Delta t}\mu_K(0) - \frac{4}{\Delta t^2}\right]$$

$$A_{35} = \sum_{K=1}^{3N} \alpha_{2K3}\left[\frac{2}{\Delta t}\mu_K(0) - \frac{4}{\Delta t^2}\right]$$

$$A_{41} = \sum_{K=1}^{3N} \alpha_{1K4}\left[\frac{2}{\Delta t}\mu_K(0) - \frac{4}{\Delta t^2}\right]$$

$$A_{42} = \frac{2}{\Delta t}\sum_{K=1}^{3N} \alpha_{3K4}\mu_K(0)$$

$$A_{43} = \sum_{K=1}^{3N} \beta_{1K4}\left[\frac{2}{\Delta t}\mu_K(0) - \frac{4}{\Delta t^2}\right]$$

$$A_{44} = \frac{4}{\Delta t^2} I_{ty} + \frac{2}{\Delta t}\sum_{K=1}^{3N} \beta_{3K4}\mu_k(0) + K_{\phi y}\left[0.55 + \frac{2}{\Delta t}0.36\left(\frac{r}{c_s}\right) + \frac{4}{\Delta t^2}0.023\left(\frac{r}{c_s}\right)^2 + \frac{\Delta t}{2}0.563\left(\frac{c_s}{r}\right)\right]$$

$$A_{45} = \sum_{K=1}^{3N} \alpha_{2K4}\left[\frac{2}{\Delta t}\mu_K(0) - \frac{4}{\Delta t^2}\right]$$

$$A_{51} = \sum_{K=1}^{3N} \alpha_{1K5}\left[\frac{2}{\Delta t}\mu_K(0) - \frac{4}{\Delta t^2}\right]$$

$$A_{52} = \sum_{K=1}^{3N} \alpha_{3K5}\left[\frac{2}{\Delta t}\mu_K(0) - \frac{4}{\Delta t^2}\right]$$

$$A_{53} = \sum_{K=1}^{3N} \beta_{1K5}\left[\frac{2}{\Delta t}\mu_K(0) - \frac{4}{\Delta t^2}\right]$$

$$A_{54} = \sum_{K=1}^{3N} \beta_{3K5}\left[\frac{2}{\Delta t}\mu_K(0) - \frac{4}{\Delta t^2}\right]$$

$$A_{55} = \frac{4}{\Delta t^2}\left(\frac{1}{r_0}\right)\left[m_0 r_0^2 + \sum_{i=1}^{N} m_i r_i^2\right] + \sum_{K=1}^{3N} \alpha_{3K2}\left[\frac{2}{\Delta t}\mu_K(0) - \frac{4}{\Delta t^2}\right] + \left(\frac{K_{U\theta}}{r_0}\right)\left[0.575 + \frac{2}{\Delta t}0.292\left(\frac{r}{c_s}\right) + \frac{\Delta t}{2}0.619\left(\frac{c_s}{r}\right)\right]$$

$$B_1 = -m_0 \ddot{U}_{gx}(t_n) + m_0 \hat{Y}_3(U_{0x}) + \sum_{K=1}^{3N} \alpha_{1K1}\left[-\frac{\Delta t}{2}\ddot{U}_{gx}(t_n)\mu_K(0) + \frac{\Delta t}{2}\hat{Y}_3(U_{0x})\mu_K(0) - \hat{Y}_1\{(\ddot{U}_{gx} + \ddot{U}_{0x})\mu_K\}\right] + \sum_{K=1}^{3N} \beta_{1K1}\left[\frac{\Delta t}{2}\hat{Y}_3(\Phi_{0x})\mu_K(0) - \hat{Y}_1(\ddot{\Phi}_{0x}\mu_K)\right] + r_0\sum_{K=1}^{3N} \alpha_{2K1}\left[\frac{\Delta t}{2}\hat{Y}_3(U_{0\theta})\mu_K(0) - \hat{Y}_1(\ddot{U}_{0\theta}\mu_K) - \hat{Y}_3(U_{0\theta})\right] + \sum_{K=1}^{3N} \alpha_{3K1}\left[-\frac{\Delta t}{2}\ddot{U}_{gy}(t_n)\mu_K(0) + \frac{\Delta t}{2}\hat{Y}_3(U_{0y})\mu_K(0) - \hat{Y}_1\{(\ddot{U}_{gy} + \ddot{U}_{0y})\mu_K\} + \ddot{U}_{gy}(t_n) - \hat{Y}_3(U_{0y})\right] + \sum_{K=1}^{3N} \beta_{3K1}\left[\frac{\Delta t}{2}\hat{Y}_3(\Phi_{0y})\mu_K(0) - \hat{Y}_1(\ddot{\Phi}_{0y}\mu_K) - \hat{Y}_3(\Phi_{0y})\right] + 0.6K_{Ux}\left(\frac{r}{c_s}\right)\hat{Y}_2(U_{0x})$$

$$B_2 = -m_0 \ddot{U}_{gy}(t_n) + m_0 \hat{Y}_3(U_{0y}) + \sum_{K=1}^{3N} \alpha_{1K2}\left[-\frac{\Delta t}{2}\ddot{U}_{gy}(t_n)\mu_K(0) + \frac{\Delta t}{2}\hat{Y}_3(U_{0x})\mu_K(0) - \hat{Y}_1\{(\ddot{U}_{gy} + \ddot{U}_{0y})\mu_K\} + \ddot{U}_{gx}(t_n) - \hat{Y}_3(U_{0x})\right] + \sum_{K=1}^{3N} \beta_{1K2}\left[\frac{\Delta t}{2}\hat{Y}_3(\Phi_{0y})\mu_K(0) - \hat{Y}_1(\ddot{\Phi}_{0y}\mu_K) - \hat{Y}_3(\Phi_{0y})\right] + r_0\sum_{K=1}^{3N} \alpha_{2K2}\left[\frac{\Delta t}{2}\hat{Y}_3(U_{0\theta})\mu_K(0) - \hat{Y}_1(\ddot{U}_{0\theta}\mu_K) - \hat{Y}_3(U_{0\theta})\right] + \sum_{K=1}^{3N} \times \alpha_{3K2}\left[-\frac{\Delta t}{2}\ddot{U}_{gy}(t_n)\mu_K(0) + \frac{\Delta t}{2}\hat{Y}_3(U_{0y})\mu_K(0) - \hat{Y}_1\{(\ddot{U}_{gy} + \ddot{U}_{0y})\mu_K\}\right] + \sum_{K=1}^{3N} \beta_{3K2}\left[\frac{\Delta t}{2}\hat{Y}_3(\Phi_{0y})\mu_K(0) - \hat{Y}_1(\ddot{\Phi}_{0y}\mu_K)\right] + 0.6K_{Uy}\left(\frac{r}{c_s}\right)\hat{Y}_2(U_{0y})$$

$$B_3 = I_{tx}\hat{Y}_3(\Phi_{0x}) + \sum_{K=1}^{3N} \alpha_{1K3}\left[-\frac{\Delta t}{2}\ddot{U}_{gx}(t_n)\mu_K(0) + \frac{\Delta t}{2}\hat{Y}_3(U_{0x})\mu_K(0) - \hat{Y}_1\{(\ddot{U}_{gx} + \ddot{U}_{0x})\mu_K\}\right] + \sum_{K=1}^{3N} \beta_{1K3}\left[\frac{\Delta t}{2}\hat{Y}_3(\Phi_{0x})\mu_K(0) - \hat{Y}_1(\ddot{\Phi}_{0x}\mu_K)\right] + r_0\sum_{K=1}^{3N} \alpha_{2K3}\left[\frac{\Delta t}{2}\hat{Y}_3(U_{0\theta})\mu_K(0) - \hat{Y}_1(\ddot{U}_{0\theta}\mu_K) - \hat{Y}_3(U_{0\theta})\right]$$

$$+\sum_{K=1}^{3N}\alpha_{3K3}\left[-\frac{\Delta t}{2}\ddot{U}_{gy}(t_n)\mu_K(0)+\frac{\Delta t}{2}\hat{Y}_3(U_{0y})\mu_K(0)\right.$$

$$\left.-\hat{Y}_1\{(\ddot{U}_{gy}+\ddot{U}_{0y})\mu_K\}+\ddot{U}_{gy}(t_n)-\hat{Y}_3(U_{0y})\right]$$

$$+\sum_{K=1}^{3N}\beta_{3K3}\left[\frac{\Delta t}{2}\hat{Y}_3(\Phi_{0y})\mu_K(0)-\hat{Y}_1(\ddot{\Phi}_{0y}\mu_K)\right.$$

$$\left.-\hat{Y}_3(\Phi_{0y})\right]+K_{\phi x}\left[0.36\left(\frac{r}{c_s}\right)\hat{Y}_2(\Phi_{0x})\right.$$

$$\left.+0.023\left(\frac{r}{c_s}\right)^2\hat{Y}_3(\Phi_{0x})-0.563\left(\frac{c_s}{r}\right)\hat{Y}_1(\Phi_{0x}\eta_\phi)\right]$$

$$B_4=I_{ty}\hat{Y}_3(\Phi_{0y})$$

$$+\sum_{K=1}^{3N}\alpha_{1K4}\left[-\frac{\Delta t}{2}\ddot{U}_{gx}(t_n)\mu_K(0)+\frac{\Delta t}{2}\hat{Y}_3(U_{0x})\mu_K(0)\right.$$

$$\left.-\hat{Y}_1\{(\ddot{U}_{gx}+\ddot{U}_{0x})\mu_K\}+\ddot{U}_{gx}(t_n)-\hat{Y}_3(U_{0x})\right]$$

$$+\sum_{K=1}^{3N}\beta_{1K4}\left[\frac{\Delta t}{2}\hat{Y}_3(\Phi_{0x})\mu_K(0)-\hat{Y}_1(\ddot{\Phi}_{0x}\mu_K)\right.$$

$$\left.-\hat{Y}_3(\Phi_{0x})\right]+r_0\sum_{K=1}^{3N}\alpha_{2K4}\left[\frac{\Delta t}{2}\hat{Y}_3(U_{00})\mu_K(0)\right.$$

$$\left.-\hat{Y}_1(\ddot{U}_{00}\mu_K)-\hat{Y}_3(U_{00})\right]+\sum_{K=1}^{3N}$$

$$\times\alpha_{3K4}\left[-\frac{\Delta t}{2}\ddot{U}_{gy}(t_n)\mu_K(0)+\frac{\Delta t}{2}\hat{Y}_3(U_{0y})\mu_K(0)\right.$$

$$\left.-\hat{Y}_1\{(\ddot{U}_{gy}+\ddot{U}_{0y})\mu_K\}\right]+\sum_{K=1}^{3N}\beta_{3K4}\left[\frac{\Delta t}{2}\hat{Y}_3(\Phi_{0y})\mu_K(0)\right.$$

$$\left.-\hat{Y}_1(\ddot{\Phi}_{0y}\mu_K)\right]+K_{\phi y}\left[0.36\left(\frac{r}{c_s}\right)\hat{Y}_2(\Phi_{0y})\right.$$

$$\left.+0.023\left(\frac{r}{c_s}\right)^2\hat{Y}_3(\Phi_{0y})-0.563\left(\frac{c_s}{r}\right)\hat{Y}_1(\Phi_{0y}\eta_\phi)\right]$$

$$B_5=\left[m_0r_0^2+\sum_{i=1}^{N}m_ir_i^2\right]\hat{Y}_3(U_{00})$$

$$+\sum_{K=1}^{3N}\alpha_{1K5}\left[-\frac{\Delta t}{2}\ddot{U}_{gx}(t_n)\mu_K(0)+\frac{\Delta t}{2}\hat{Y}_3(U_{0x})\mu_K(0)\right.$$

$$\left.-\hat{Y}_1\{(\ddot{U}_{gx}+\ddot{U}_{0x})\mu_K\}+\ddot{U}_{gx}(t_n)-\hat{Y}_3(U_{0x})\right]$$

$$+\sum_{K=1}^{3N}\beta_{1K5}\left[\frac{\Delta t}{2}\hat{Y}_3(\Phi_{0x})\mu_K(0)-\hat{Y}_1(\ddot{\Phi}_{0x}\mu_K)\right.$$

$$\left.-\hat{Y}_3(\phi_{0x})\right]+r_0\sum_{K=1}^{3N}\alpha_{2K5}\left[\frac{\Delta t}{2}\hat{Y}_3(U_{00})\mu_K(0)\right.$$

$$\left.-\hat{Y}_1(\ddot{U}_{00}\mu_K)-\hat{Y}_3(U_{00})\right]+\sum_{K=1}^{3N}\alpha_{3K5}\left[\right.$$

$$-\frac{\Delta t}{2}\ddot{U}_{gy}(t_n)\mu_K(0)+\frac{\Delta t}{2}\hat{Y}_3(U_{0y})\mu_K(0)-\hat{Y}_1\{(\ddot{U}_{gy}$$

$$+\ddot{U}_{0y})\mu_K\}+\ddot{U}_{gy}(t_n)-\hat{Y}_3(U_{0y})\left.\right]+\sum_{K=1}^{3N}\beta_{3K5}$$

$$\times\left[\frac{\Delta t}{2}\hat{Y}_3(\Phi_{0y})\mu_K(0)-\hat{Y}_1(\ddot{\Phi}_{0y}\mu_K)-\hat{Y}_3(\Phi_{0y})\right]$$

$$+K_{U0}\left[0.292\left(\frac{r}{c_s}\right)\hat{Y}_2(U_{00})-0.619\left(\frac{c_s}{r}\right)\hat{Y}_1(U_{00}\eta_\theta)\right],$$

where $\mu_K$ are as defined at the end of eqns (6), and

$$\eta_\phi=e^{-1.25(c_s/r)(t_n-t_i)}\quad\text{and}\quad\eta_\theta=e^{-1.456(c_s/r)(t_n-t_i)}.$$

$\hat{Y}_1$, $\hat{Y}_2$, and $\hat{Y}_3$ are operators given by

$$\hat{Y}_1(\hat{x})=\frac{\Delta t}{2}\hat{x}(t_0)+\Delta t\sum_{j=1}^{n-1}\hat{x}(t_j),$$

$$\hat{Y}_2(\hat{x})=\frac{2}{\Delta t}\hat{x}(t_{n-1})+\dot{\hat{x}}(t_{n-1})$$

$$\hat{Y}_3(\hat{x})=\frac{4}{\Delta t^2}\hat{x}(t_{n-1})+\frac{4}{\Delta t}\dot{\hat{x}}(t_{n-1})+\ddot{\hat{x}}(t_{n-1}),$$

where $\hat{x}$ is the variable.

*Numerical scheme for operator* $\hat{Y}_1$

Operator $\hat{Y}_1$ requires considerable computational effort. Direct operation at every time step is not numerically efficient. However, note that there are basically three different functions namely, $\mu_K$, $\eta_\phi$, and $\eta_\theta$ which are involved along with the footing displacements $U_{0x}$, $U_{0y}$, $\Phi_{0x}$, $\Phi_{0y}$, and $U_{00}$. Since, these functions involve cosine and exponential functions it is possible to develop recurrence formulae [10, 11], which greatly reduce the computational effort.